

Theoretical study of the solvent effects on electronic properties of 2(1*H*)-quinoxalinone derivatives

Tourya Ghailane¹, Rachida Ghailane^{1,*}, Khadija Marakchi², Brahim Lakhri³,
Najia Komiha² and Abdelaziz Souizi¹

¹Laboratory of Organic, Organometallic and Theoretical chemistry, Department of Chemistry, University of Ibn Tofail, Faculty of Science, Kenitra, Morocco

²LS3ME-Equipe de Chimie Théorique et Modélisation, Département de Chimie, Université Mohammed V, Faculté des Sciences B.P 1014, Rabat, Morocco

³Laboratoire d'Agroressources et Génie des Procédés, Faculté des Sciences, Université Ibn Tofail, Kénitra, Morocco

Abstract: The geometrical structures and electronic spectra of three quinoxalinone derivatives have been investigated theoretically by performing DFT and TDDFT calculations with standard basis sets containing polarization and diffuse functions. The solvent effect was taken into account using self-consistent isodensity polarized continuum model (SCIPCM); three polar solvents were considered. The effect of the solvent polarity on the geometries, solvation energies, dipole moment, the energy gap between HOMO and LUMO and UV-visible electronic transitions were examined for all studied compounds. The theoretical electronic spectrum of 2(1*H*)-quinoxalinone was compared with the experimental one. The experimental electronic spectrum recorded in ethanol exhibit three absorption bands respectively at 230, 280 and 350 nm. The existence of these bands has been confirmed by TDDFT calculations for the studied quinoxalinone derivatives. The effects of solvent polarity and the nature of the substituent of the quinoxalinone on the displacement of the calculated absorption bands are discussed.

Keywords: Quinoxalines, UV-Visible, solvent effect, TDDFT, electronic transitions.

Introduction

Quinoxaline derivatives form an important class of benzoheterocycles which has received a good deal of interest in the last years due to their both biological properties and pharmaceutical applications¹. They are widely applied for medical use as antibiotics, antidepressants, anti-convulsants²⁻⁴, anticancer⁵, antibacterial⁶, and antitumor⁷⁻¹⁰ activities. They are also used in the agricultural field, and cosmetics¹¹⁻¹⁴. Some quinoxaline derivatives act as DNA photocleavers¹⁵. The quinoxaline moiety exists in peptide antibiotics such as echinomycin and triostin A¹⁶ as well as in TANDEM which is known to intercalate bifunctionally into DNA¹⁷.

The use of the density functional theory (DFT) allows prediction of the molecular structure and spectroscopic properties as well as the tautomeric equilibria, of organic compounds¹⁸⁻²². The time dependent density functional theory (TDDFT) method has become the most widely used tool for theoretically evaluating the energies of the

excited state and to simulate the UV-vis and fluorescence spectra of organic compounds and metal complexes in solution^{23,24}. The calculations at B3LYP/6-31+G**, 6-311++G** and 6-311G** levels are employed to determine and optimize all the tautomeric forms of 2-hydroxyquinoxaline 2-OHQ. It is shown that the keto form of 2-OHQ is the most stable tautomer²⁵. The QCISD method was also used to support relative energy values. The best results are obtained at the B3LYP/ 6-311++G** level of the theory and compared with experiment. The detailed crystal data on 2-OHQ has been reported previously by N. Padjama et al.²⁶.

The spectroscopic study and conformational analysis of the 2-quinoxaline carboxylic acid (2-QCA) were performed theoretically at B3LYP/6-31G* level and experimentally by N. Prabavathi et al.²⁷. The X-ray single crystallography was used to study the solid state molecular structure of 2,3-dihydroxyquinoxaline (DHQ). The tautomerism and spectral properties of DHQ are studied in the vacuum and in the presence of different solvents using the B3LYP/6-311++G(d, p) method²⁸.

*Corresponding author : Rachida Ghailane

Email address: ghailane_r@yahoo.fr

DOI: <http://dx.doi.org/10.13171/mjc55/01606171600/ghailane>

Received April 25th, 2016

Accepted May 22nd, 2016

Published June 17th, 2016

The geometrical structure and spectroscopic properties of 3-hydroxy-2-quinoxalinecarboxylic acid (3HQC) are studied experimentally and theoretically using B3LYP/6-311++G(d, p) by S. Yurdakul et al.²⁹. Seven tautomers were determined among many stable conformations; the experimental spectra were concordant with the theoretical data of two tautomers. The authors have concluded that the stable tautomeric forms are stabilized by intramolecular O-H...O and O-H...N hydrogen bond type.

The aim of this study is to examine the effect of the solvent polarity and the effect of the introduction of polarization functions and diffuse functions in the standard basis on the geometrical structures and on the electronic spectra of the three derivatives quinoxaline. The optimized geometrical structures, the absorption wavelengths, excitations energies of three quinoxaline derivatives, 2(1H)-quinoxalinone **HQ** (Fig.1), 3-(Methyl)-2-quinoxalinone **CH₃Q** and 3-(Formyl)-2-quinoxalinone **CHOQ** (Scheme1),

have been carried out using DFT and TDDFT theories combined with standard basis sets 6-31G*, 6-31+G**, 6-311++G** and 6-311G** which are proved to be sufficient for similar studies. The use of the Time-Dependent Density Functional Theory (TDDFT) method turns out reliable for the determination of the electronic spectra^{30,31}. The choice of the four basis could be justified by the fact that in a previous study of FT-IR and TF-Raman spectra of Keto and enol forms of HQ at B3LYP// 6-31+G**//6-311++G**// 6-311G** level of theory give a good agreement theory-experiment, one also chooses to use the 4th basis set 6-31G* to check if it is sufficient to well describe the geometrical structure of the HQ. We have decided to focus our interest on the solvent polarity effects on UV-visible spectra for the three quinoxaline derivatives. On the other hand, the substitution effect was deduced by comparing the wavelengths (λ_{max}) of the maximum absorption peaks obtained from the electronic spectra of the three derivatives.

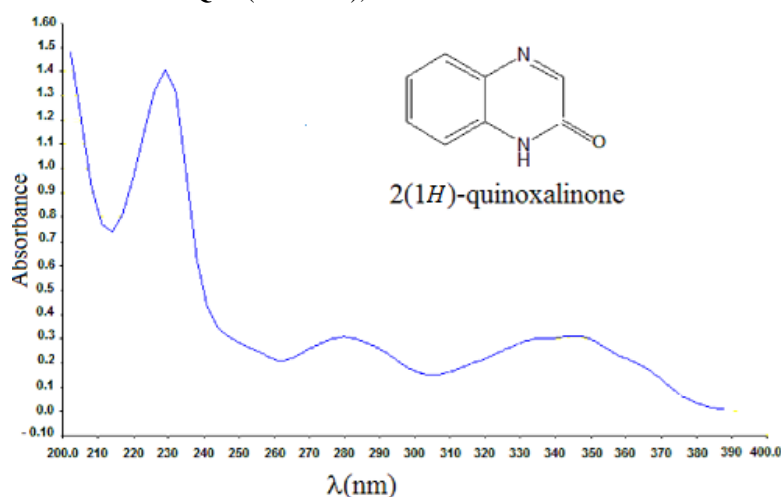
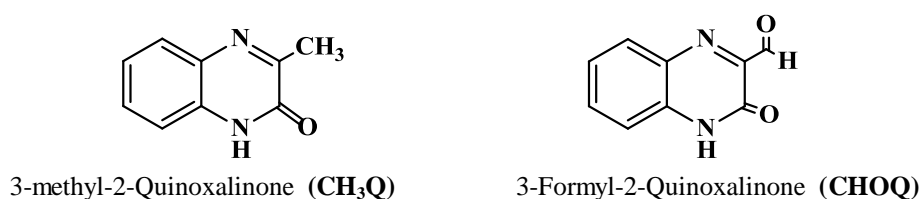


Figure 1. Experimental absorption spectrum of **HQ** in ethanol.



Scheme 1. Chemical structures of the investigated quinoxaline derivatives.

Illustration of the electronics properties of these derivative can be provided from the electronic parameter values such as dipole moment and energy gap, which were obtained using the same level of theory in the both gas and solvated phases.

Synthesis part and experimental UV spectra of 2(1H)-quinoxalinone

2(1H)-quinoxalinone **HQ** was synthesized in the laboratory of one of the authors, its synthesis

and purification methods have been described elsewhere³². Spectrograde ethanol is used as it is. Absorption spectra are observed with a spectrophotometer (Cary 5G, UV-visible-NIR).

The ultraviolet-visible spectra of 2(1H)-quinoxalinone are given in Fig. 1.

Experimental Section

Apparatus for identification of quinoxalin-2(1H)-one. ^1H NMR spectra in DMSO-d_6 was taken on Bruker WB-300, and chemical shifts given in ppm downfield from TMS and melting point was determined on melting Point Apparatus (Jencons 9200) and is uncorrected.

Synthesis of 2(1H)-quinoxalinone ³²: a mixed solution of o-phenylenediamine (2.16 g, 20 mmol) and glyoxylic acid (2.3 g, 25 mmol in n-butanol (60 mL) was refluxed for 5 hrs. After standing in a freezer for one night, the formed solid was filtered under reduced pressure and washed with cyclohexane (20 mL) to give light yellow crystal of 2(1H)-quinoxalinone (2.28 g, yield 78%; mp 236-238 °C).

Spectral data of 2(1H)-quinoxalinone ^1H NMR (DMSO-d_6), $\delta(\text{ppm})$: 12.45 (s, 1H, N-H), 7.30-7.80 (m, 4H, Ar-H), 8.18 (s, 1H, C-H).

Computational details

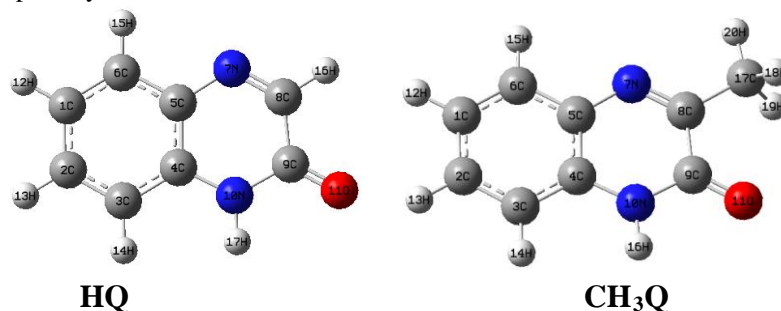
Ground-state electronic structure calculations of quinoxalinone derivatives are performed in vacuum without any symmetry constraint using the Density Functional Theory (DFT) with the Beck's three parameter exchange functional and the Lee-Yang-Parr non-local correlation functional (B3LYP) ³³⁻³⁵. This level of theory was shown to be reliable to geometric optimization and the determination of the energy parameters for a wide variety of systems. Four basis sets of atomic orbitals, 6-31G(d), 6-311G(d,p), 6-31+G(d,p) and 6-311++G(d,p) as implemented in Gaussian 03 program package ³⁶, were used throughout this study. These basis sets contain polarization functions allowing to describe correctly the intramolecular H bonding and the excited states. The stability of the optimized geometry of the molecular structure was confirmed by harmonic vibrational wavenumbers calculated using analytic second derivatives which have shown the absence of imaginary frequency modes. For all performed calculations, in this study, solvent effects were taken into account by self-consistent reaction field SCRF method using a self-consistent isodensity polarized continuum model (SCIPCM) ³⁷. Moreover, three solvents THF, ethanol (EtOH) and acetonitrile (MeCN) whose dielectric constants (ϵ) are 7.426, 24.852 and 35,688 respectively ³⁶, are considered in order to discuss the polarity effects on the electronic

parameters and the UV-visible electronic transitions for the studied molecules. Indeed, the solute-solvent interactions have a direct and significant influence on UV-visible spectra. As a consequence, a reliable theoretical study of electronic spectra cannot be performed without a proper treatment of solvation. Time-dependent density functional theory (TDDFT) calculations with B3LYP functional have been performed for quinoxaline derivatives, in the gas, and in solution, on the basis of fully optimized ground state geometrical structures in the vacuum at the same level of theory. These calculations allow us to investigate the electronic absorption properties and to get the excitation energies. Otherwise, in order to correctly reproduce the UV spectra of quinoxaline derivatives, vertical excitation energies are computed for the 30 first singlet excited states.

Results and Discussion

Molecular geometry

The Optimized geometries of studied derivatives are determined by complete optimization, in vacuum, using B3LYP functional. The geometrical structure of **HQ** (Fig.2) has been already optimized with B3LYP method using 6-311++G(d, p), 6-31+G(d, p) and 6-311G(d, p) basis sets, it is shown that the keto form of 2-OHQ is the most stable tautomère ²⁵. In the present work, the standard basis 6-31G(d) was also used in order to verify whether it is possible to better describe the geometrical structure of this molecule while reducing the computational cost. The complete geometrical optimization of **CH₃Q** and **CHOQ** derivatives (Fig. 2) were carried out using B3LYP combined with the four standard basis 6-31G(d) (B), 6-311G(d,p) (B2), 6-31+G(d,p) (B1) and 6-311++G(d,p) (B3) in vacuum. For each optimized structure, the calculation of the vibrational frequencies was performed and shows that there is no imaginary frequency. Consequently, each geometrical structure corresponds to a stationary point on the potential energy surface. The optimized structures of three derivatives with the label of atoms are presented in Fig. 2. Moreover, the exact values of some selected bond lengths and bond angles of these derivatives were collected in Table 1. In the literature, there are no exact X-ray crystal structures for **CH₃Q** and **CHOQ** molecules; thus, they are compared with the experimental data of the **HQ** molecule ²⁶.



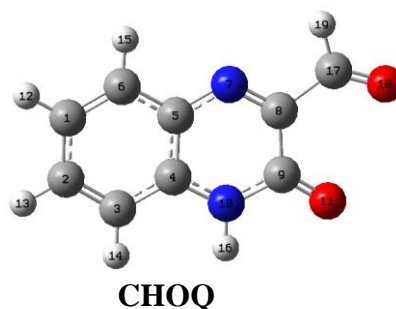


Figure 2. Optimized molecular structures of quinoxalinone derivatives.

Table 1. Bond length (Å) and Bond angle (°) of the studied quinoxaline derivatives **HQ**, **CH₃Q** and **CHOQ** calculated at B3LYP using four basis sets 6-31G(d) (B), 6-311G(d,p) (B2), 6-31+G(d,p) (B1) and 6-311++G(d,p) (B3) in gas phase.

Basis sets	HQ		CH ₃ Q			CHOQ			HQ	
	B	B	B2	B1	B3	B	B2	B1	B3	X-Ray ^[26]
Bond length										
(Å)	1.404	1.404	1.402	1.406	1.402	1.407	1.409	1.409	1.405	1.403
C1-C2	1.389	1.389	1.386	1.390	1.387	1.388	1.389	1.389	1.385	1.363
C2-C3	1.402	1.402	1.400	1.403	1.400	1.403	1.405	1.405	1.402	1.401
C3-C4	1.416	1.414	1.411	1.414	1.411	1.419	1.419	1.419	1.415	1.411
C4-C5	1.405	1.405	1.403	1.407	1.404	1.409	1.411	1.410	1.408	1.381
C5-C6	1.387	1.387	1.384	1.389	1.385	1.384	1.385	1.385	1.492	1.375
C6-C1	1.481	1.492	1.493	1.493	1.493	1.491	1.492	1.492	1.373	1.398
C8-C9	1.383	1.383	1.382	1.384	1.383	1.376	1.377	1.377	1.299	1.212
C4-N10	1.389	1.388	1.387	1.388	1.386	1.375	1.375	1.375	2.275	1.386
C5-N7	1.390	1.385	1.383	1.382	1.382	1.400	1.397	1.397	2.451	1.342
C9-N10	1.292	1.296	1.292	1.298	1.293	1.303	1.304	1.304		1.287
C8-N7	1.223	1.225	1.219	1.229	1.221	1.217	1.220	1.220		1.239
C9-O11	2.293	2.286	2.280	2.284	2.279	2.280	2.275	2.279		
N10...O11	2.490	2.475	2.471	2.472	2.471	2.452	2.450	2.450		
H16...O11										
Bond angle (°)										
C2C1C6	119.8	119.8	119.8	119.9	119.9	119.7	119.7	119.8	119.8	120.0
C3C4C5	120.3	120.5	120.4	120.6	120.5	120.1	120.0	120.2	120.1	119.4
C1C2C3	120.9	120.8	120.8	120.7	120.7	121.2	121.2	121.2	121.2	120.8
C4C5C6	119.1	118.9	118.9	118.9	118.9	119.3	119.3	119.4	119.4	119.4
C6C5N7	119.4	119.4	119.5	119.5	119.5	119.6	119.6	119.6	119.7	119.2
C3C4N10	122.4	122.5	122.6	122.5	122.5	122.8	122.8	122.8	122.8	122.3
C4N10C9	124.3	124.4	124.4	124.4	124.4	125.4	125.3	125.3	125.3	122.5
C5N7C8	118.6	119.7	119.9	120.1	120.1	120.4	120.7	120.7	120.8	117.5
N10C9O11	122.5	122.1	122.2	121.9	122.1	121.0	120.9	120.9	121.1	121.8
C8C9O11	124.7	124.2	124.2	124.1	124.1	126.9	126.7	126.7	126.7	122.6

The geometrical parameters values calculated at B3LYP/6-31G(d) level of theory was shown to be in good agreement with the experimental data of **HQ**. Therefore, the use of this level of theory seems to be sufficient to correctly describe the geometrical structure of similar molecules. The geometrical structure of benzenic cycle of quinoxaline was weakly affected by the substitution of H in **HQ** molecule by CH₃ or CHO. The bond lengths presented in Table 1 are generally longer than those obtained by X-ray. The larger deviations of the

calculated values from the experimental data are 0.028 Å and 0.056 Å observed respectively for C8-C9 and C9-N10. While the value of the bond length C9-O11 is shorter than that given by the experiment of about 0.027 Å.

In the benzene ring, C2C1C6 and C4C5C6 bond angles are slightly smaller than 120 and C1C2C3 and C3C4C5 are slightly larger than 120. The value of the bond angle in the benzene ring is between 119.7 and 120.4°. On the other side, within the heterocyclic ring, the bond angles vary between 119.5° and

124.4° for **CH₃Q** and 119.7° and 125.3° for **CHOQ**. The larger deviation from the experience was 2.8° observed for the C4N10C9 bond angle calculated using 6-311++G (d, p) (B3) basis for **CHOQ**. For the bond angle outside the heterocyclic ring, the bond angle C8C9O11 for **CHOQ** is larger by 4.1° than the experiment.

Both molecules **HQ** and **CHOQ** are planar, all dihedral angle values are equal to 0 or 180°; whereas, this planarity is broken by the presence of the CH₃ substituent in the case of **CH₃Q** derivative. The structural analysis reveals the presence of weak intermolecular hydrogen bond interactions between O11...H16-N10 in the studied molecules. The distance between O11...N10 is about 2.29 Å, this value is < 3.0 Å in accordance of a hydrogen interaction³⁸. The values of the hydrogen bond (O11...H16-N10) observed in the three molecules **CHOQ**, **CH₃Q** and **HQ** are respectively 2.49Å, 2.47Å and 2.45Å, values are in good agreement with the value 2.478 Å given by S. Sudha et al³⁹ for an intramolecular C-H...O hydrogen bond, observed in the dibenzalacetone (DBA) molecule, between oxygen atom of C=O group and hydrogen atom of alkene group. We can notice that a slight increase of interaction observed in **CHOQ** molecule is translated by the shorter hydrogen bond. The table 1 shows that the values of hydrogen bond remain almost constant for the three quinoxaline derivatives, by adding the diffuse function in the basis sets of atomic orbitals.

Solvation energy and electronics parameters

The solvation energy (ΔE_{sol}) is estimated by the difference between the total energy obtained in the

solvent and that calculated in vacuum, it is defined as following:

$$\Delta E_{\text{sol}} = E_{\text{T}}(\text{in solution}) - E_{\text{T}}(\text{in vacuum})$$

The solvation energies reported in Table 2 show that the calculations, using 6-31+G(d,p) basis, lead to a better stabilization for the three derivatives. The ΔE_{sol} values are the largest one for the most polar solvent MeCN compared to those obtained in EtOH and THF solvents. In the presence of the solvent, this stabilization is less important when the H in the position α to keto is substituted by CH₃ group rather than by CHO substituent. One can also notice that the polarity of the solvent increases the solvation energy and the difference between the ΔE_{sol} values obtained in THF and MeCN solvents, using 6-31+G(d,p) (B1) basis, is about 2 kcal for **CHOQ** and 1kcal for **CH₃Q** and **HQ**. To conclude, the most important stabilization caused by the solvent polarity effects is observed for **CHOQ**. It is well known that the solvent interact with the polarized bond and its effect is more important when the molecule contains more polarized bonds, and **CHOQ** contains two C=O groups strongly polarized. Furthermore, considering the ΔE_{sol} values obtained with MeCN using 6-31+G(d,p) (B1) basis, the difference between ΔE_{sol} values of **CHOQ** and that of **HQ** is equal to 3.74kcal, while the difference between ΔE_{sol} values of **CH₃Q** and that of **HQ** is equal to -0.78 kcal. One can deduce that when we replace H by an electro-donor group like CH₃, the solvation energy decreases, conversely the substitution of H by an electro-attractor group CHO leads to an increase of the solvation energy.

Table 2. Total energies (in a.u) and solvation energy ΔE_{sol} (in kcal) of the three quinoxaline derivatives.

Basis	phase	HQ		CH ₃ Q		CHOQ	
		E(a.u)	ΔE_{sol}	E(a.u)	ΔE_{sol}	E(a.u)	ΔE_{sol}
6-31G(d)	Gas	-493.203959	---	-532.528622	---	-606.519292	---
	THF	-493.212961	5.65	-532.537019	5.27	-606.532440	8.26
	EtOH	-493.214541	6.64	-532.538547	6.23	-606.534838	9.75
	MeCN	-493.214792	6.80	-532.538792	6.39	-606.535222	9.99
6-311G(d,p)	Gas	-493.328046	---	-532.663287	---	-606.673760	---
	THF	-493.336859	5.53	-532.671314	5.03	-606.686661	8.09
	EtOH	-493.338404	6.50	-532.672762	5.95	-606.689012	9.57
	MeCN	-493.338649	6.66	-532.672994	6.09	-606.689388	9.80
6-31+G(d,p)	Gas	-493.235650	---	-532.563418	---	-606.554619	---
	THF	-493.245144	5.95	-532.571823	5.28	-606.568943	8.99
	EtOH	-493.246817	7.01	-532.573344	6.23	-606.571588	10.65
	MeCN	-493.247083	7.17	-532.573587	6.39	-606.572014	10.91
6-311++G(d,p)	Gas	-493.337877	---	-532.672462	---	-606.685597	---
	THF	-493.347197	5.86	-532.680733	5.19	-606.699508	8.72
	EtOH	-493.348837	6.87	-532.682233	6.13	-606.702071	10.33
	MeCN	-493.349098	7.03	-532.682474	6.27	-606.702482	10.61

6-31G(d) ; 6-311G(d,p) ; 6-31+G(d,p) and 6-311++G(d,p) correspond, in the text, to B; B2; B1 and B3 respectively.

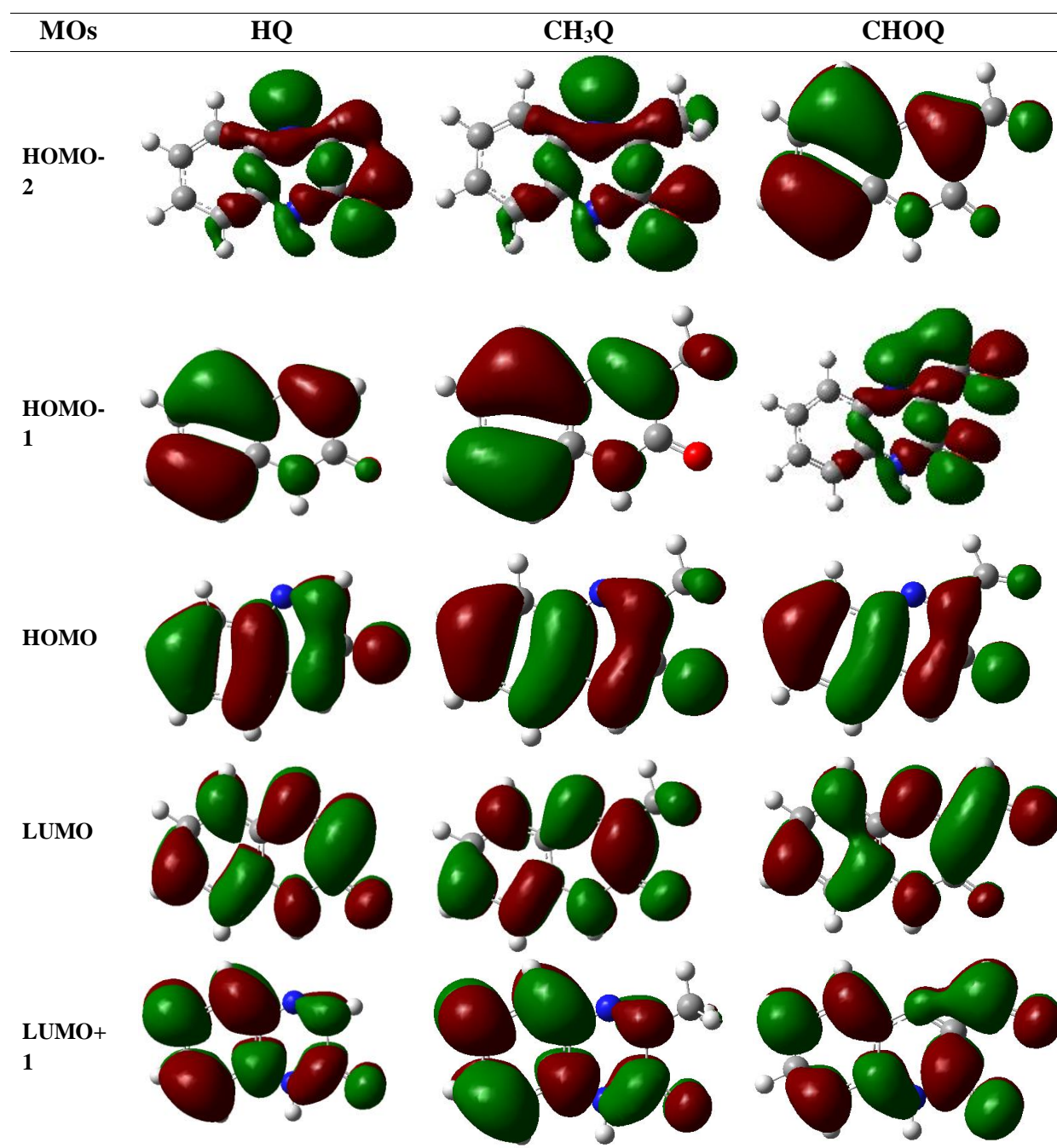


Figure 3. Isodensity plots of the frontier orbitals of the quinoxalines derivatives.

The dipole moment and energy gap between HOMO and LUMO are often used to discuss the physical and chemical behavior of molecular system such as activity, reactivity, optical and electrical properties. Table 3 shows that the largest dipole moment values are given with the calculations using 6-31+G (d, p) (B1) basis for the three derivatives and the dipole moment values in a solvent are larger than that in a vacuum, and, they increase with the solvent polarity. The solvent effect on the dipole moment is notable for **CHOQ**, this can be shown by the difference, between the values obtained in gas and in MeCN (the most polar solvent), which is approximately 2.5D, while this difference is evaluated to 1.1 and 1.3 D for **HQ** and **CH₃Q** respectively. Moreover, the dipole moment value for

CHOQ is the largest one (10.08D) by comparison with 5.02 and 4.44 D values obtained for **HQ** and **CH₃Q** respectively.

According to the frontier molecular orbital (FMO) theory, the formation of a transition state is due to an interaction between the frontier orbitals (HOMO and LUMO) of reactants⁴⁰. The energy of the HOMO is directly related to the ionization potential and the energy of the LUMO is directly related to the electron affinity. The high value of HOMO energy is likely to indicate a tendency of the molecule to donate electrons to appropriate acceptor molecule of low empty molecular orbital energy. A low value of LUMO energy shows more probability to accept electrons. So, the gap energy, i.e. the

difference in energy between the HOMO and LUMO, is an important stability index. It is a critical parameter in determining molecular electrical transport properties because it is a measure of electron conductivity. Low gap value refers to the higher electronic transition and vice versa. The energy gap is reported in Table 3 and the LUMO and HOMO plot are shown in Fig. 3. The HOMO has a pronounced π character localized on π -system of quinoxaline moiety and the oxygen atom of carbonyl group while the LUMO has antibonding π character localized mostly on N-C and N-H bonds in the heterocyclic ring, benzene and oxygen atom of C=O group. The smaller energy gap values (Table 3) are calculated with B1 basis for the three quinoxaline derivatives in vacuum and in solution. For the studied quinoxaline derivatives, the HOMO-LUMO gap of quinoxaline derivatives in a polar solvent are smaller than that in the vacuum, this indicates that the solvent polarity effects stabilize the LUMO and destabilize the HOMO. In the MeCN polar solvent, the energy gap is equal to 3.67eV, lower than the energy gap 4.39 and 4.28 eV obtained respectively for **CH₃Q** and **HQ**. This result indicates that the transitions from the ground state to excited states are easier in **CHOQ** molecule than in **CH₃Q** and **HQ**. Therefore, the substitution effect plays an important role in molecular electrical transport properties.

UV-Vis spectra analysis

UV-visible absorption spectra of the quinoxaline derivatives were calculated by the TDDFT method in

three polar solvents to predict the effect of solvent on the absorption intensities as well as on the corresponding wavelengths values.

The time-dependent density functional method is able to reproduce the absorption wavelengths which correspond to vertical electronic transitions computed on the ground state geometry, the solvent effect could also be studied⁴¹⁻⁴³. In the present study, the TDDFT calculations were performed using B3LYP function and different standard basis set 6-31G(d), 6-31+G(d, p), 6-311++G(d, p), 6-311G(d, p) in order to determine the Low-lying excited states of the studied molecules. In these calculations, we started from the gas phase optimized geometries of the **HQ**, **CH₃Q** and **CHOQ** derivatives using the same level of theory. The three derivatives were considered so that the effect of electro-donor or electro-acceptor of the substituent group on the absorption spectrum can be discussed. The absorption wavelengths (λ_{max}), oscillator strengths (f), excitation energies (ΔE) and dominant coefficient of the excitation, in the vacuum and in the solution, are calculated for the three derivatives are regrouped in Tables 4-6. The electronic spectra are illustrated in Fig. 4 (a, b, c). Only the three first vertical excitations were considered, the corresponding oscillator strengths are greater than 0.08, 0.1 and 0.07 for **HQ**, **CH₃Q** and **CHOQ** derivatives respectively.

Table 3. Dipole moment μ (in Debye), energy gap ΔE (HOMO-LUMO) (in eV) of the three quinoxaline derivatives.

Basis	phase	HQ		CH ₃ Q		CHOQ	
		μ	ΔE	μ	ΔE	μ	ΔE
6-31G(d)	Gas	3.9807	4.364	3.1210	4.462	6.9851	3.779
	THF	5.0226	4.338	4.0364	4.442	8.9477	3.717
	EtOH	5.2028	4.330	4.1992	4.437	9.2891	3.699
	MeCN	5.2314	4.329	4.2252	4.435	9.3433	3.697
6-311G(d,p)	Gas	3.9240	4.365	3.0645	4.472	6.9170	3.799
	THF	5.2579	4.331	3.9199	4.454	8.8441	3.744
	EtOH	5.1122	4.334	4.0714	4.450	9.1783	3.728
	MeCN	5.1400	4.333	4.0955	4.449	9.2312	3.725
6-31+G(d,p)	Gas	4.3343	4.319	3.3325	4.420	7.5377	3.775
	THF	5.4129	4.293	4.2518	4.402	9.6559	3.691
	EtOH	5.5960	4.286	4.4142	4.398	10.0205	3.674
	MeCN	5.6251	4.285	4.4400	4.397	10.0783	3.671
6-311++G(d,p)	Gas	4.2453	4.330	3.2392	4.434	7.3873	3.801
	THF	5.4129	4.293	4.1262	4.416	9.4427	3.716
	EtOH	5.5960	4.286	4.2851	4.412	9.7958	3.670
	MeCN	5.4953	4.295	4.3104	4.411	9.8518	3.697

6-31G(d) ; 6-311G(d,p) ; 6-31+G(d,p) and 6-311++G(d,p) correspond, in the text, to B; B2; B1 and B3 respectively.

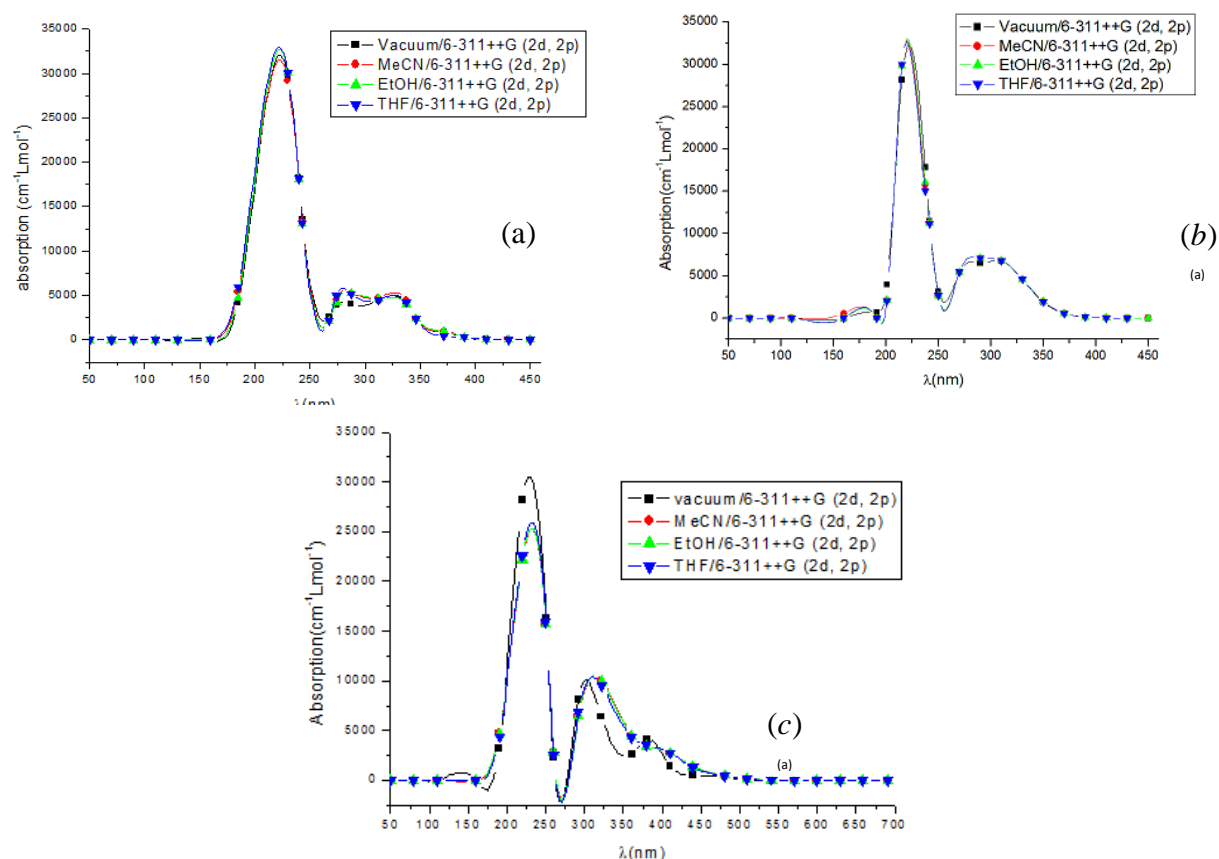


Fig. 4. Calculated electronic absorption spectra of **HQ** (a), **CH₃Q** (b) and **CHOQ** (c).

Table 4 summarized the results of the calculated vertical excitation energies of **HQ** in vacuum and in solution using TD-B3LYP method combined with four standard basis B, B2, B1 and B3. The comparison, between the wavelengths values, λ_{\max} obtained in vacuum with the different basis (Table 4) and those collected from the experimental spectrum of **HQ** which are located about 230, 280 and 350nm, shows that both B1 and B3 basis give a better approach to the experiment with λ_{\max} (222, 275 and 322nm) than that given to the basis B and B2 with λ_{\max} values (216, 269 and 316nm) and (217, 270, and 318nm) respectively. Thereby, if 6-31G*(B) is sufficient to describe correctly the geometrical structure the addition of the diffuse functions in the basis seem to be necessary to better reproduce the electronic spectrum. From Table 4, the calculated vertical excitation energies of **HQ** using TD-B3LYP with and B and B2 are (5.74, 4.60 and 3.91) and (5.70, 4.59 and 3.90 eV) respectively, these results were shown to be overestimated the experimental ones (5.39, 4.43 and 3.54eV) by (0.35, 0.17 and 0.37 eV) and (0.31, 0.16 and 0.36) for B and B2 respectively. The calculated vertical excitation energies of **HQ** with TD-B3LYP combined with B1 or B3 (5.59, 4.51 and 3.85 eV) were shown to be overestimated the experimental ones 5.39, 4.43 and 3.54 eV by only 0.2, 0.08 and 0.31 eV respectively. Therefore, the use of the basis containing diffuse functions improves the results and allows to obtain a better approach theory-experiment concerning the

determination of the vertical excitation energies than the use of basis set without diffuse functions. In the three solvents (THF, EtOH and MeCN) the results show that the better approach theory-experiment for the evaluation of vertical excitation energies is obtained using TD-B3LYP combined with B1 and B3 basis. Indeed, the use of TD-B3LYP/B3 method in THF, the evaluated vertical excitation energies are 5.60, 4.44 and 3.83 eV, the first and the third excitation energies were shown to be overestimated the experimental values by 0.21 and 0.29 eV respectively, while a weak underestimation by 0.01 eV is observed for the second excitation energy. On the other hand, in EtOH and MeCN, the calculated excitation energies are identical 5.60, 4.42 and 3.82 eV, the obtained differences between the calculated excitation energies and the experimental values are the same of that evaluated in THF. Therefore, the effect of polarity solvent on the excitation energies seems to be negligible. From the above discussion, it is noteworthy that the observed overestimation of the vertical excitation energy shows that it still remains some discrepancy between theory and experiment for **HQ**. This discrepancy can be explained by the fact that TD-B3LYP fail to reproduce the experimentally estimated excitation energies. However, to remedy this drawback, recent research works were shown that both methods TD-LC-BLYP⁴⁴ and TD-CAM-B3LYP⁴⁵ on the basis of the Bear's method⁴⁶⁻⁴⁷ are found to well reproduce the experimental excitation energies.

Table 4. Energies gap ΔE (eV) ($\Delta E = E_{\text{LUMO}} - E_{\text{HOMO}}$), calculated absorption wavelengths λ (nm) of **HQ** in gas phase and in solution. Only the three first transitions with an oscillator strength (f) > 0.03 and CI expansion coefficient > 40% are reported.

HQ	Basis set	Excitations	ΔE (eV)	λ (nm)	f	CI expansion coefficient
Gas	6-31G(d)	HOMO→LUMO	3.9128	316.87	0.0973	0.63126
		HOMO-2→LUMO	4.6030	269.36	0.0931	0.61451
		HOMO→LUMO+1	5.7445	215.83	0.3482	0.50421
	6-311G(d,p)	HOMO→LUMO	3.8977	318.09	0.0994	0.63371
		HOMO-2→LUMO	4.5903	270.10	0.0940	0.61393
		HOMO→LUMO+1	5.7004	217.50	0.3725	0.49654
	6-31+G(d,p)	HOMO→LUMO	3.8493	322.10	0.1040	0.63374
		HOMO-2→LUMO	4.5076	275.06	0.1041	0.61710
		HOMO→LUMO+1	5.5897	221.81	0.4062	0.48303
	6-311++G(d,p)	HOMO→LUMO	3.8528	321.80	0.1029	0.63454
		HOMO-2→LUMO	4.5120	274.79	0.1029	0.61743
		HOMO→LUMO+1	5.5879	221.88	0.3924	0.47960
THF	6-31G(d)	HOMO→LUMO	3.8869	318.98	0.0895	0.62938
		HOMO-2→LUMO	4.5244	274.04	0.1082	0.61811
		HOMO→LUMO+1	5.7597	215.26	0.3550	0.55460
	6-311G(d,p)	HOMO→LUMO	3.8750	319.96	0.0920	0.63210
		HOMO-2→LUMO	4.5182	274.41	0.1092	0.61876
		HOMO→LUMO+1	5.7127	217.03	0.3753	0.54835
	6-31+G(d,p)	HOMO→LUMO	3.8236	324.26	0.0949	0.63178
		HOMO-1→LUMO	4.4294	279.91	0.1215	0.62069
		HOMO→LUMO+1	5.6013	221.35	0.4123	0.55181
	6-311++G(d,p)	HOMO→LUMO	3.8264	324.02	0.0942	0.63271
		HOMO-1→LUMO	4.4370	279.43	0.1194	0.62122
		HOMO→LUMO+1	5.5983	221.47	0.3960	0.54953
EtOH	6-31G(d)	HOMO→LUMO	3.8799	319.56	0.0880	0.62923
		HOMO-2→LUMO	4.5118	274.80	0.1099	0.61827
		HOMO→LUMO+1	5.7617	215.19	0.3573	0.56098
	6-311G(d,p)	HOMO→LUMO	3.8684	320.50	0.0906	0.63198
		HOMO-2→LUMO	4.5065	275.13	0.1110	0.61909
		HOMO→LUMO+1	5.7140	216.98	0.3773	0.55520
	6-31+G(d,p)	HOMO→LUMO	3.8164	324.87	0.0931	0.63166
		HOMO-1→LUMO	4.4173	280.68	0.1234	0.62081
		HOMO→LUMO+1	5.6021	221.32	0.4153	0.56026
	6-311++G(d,p)	HOMO→LUMO	3.8192	324.63	0.0925	0.63258
		HOMO-1→LUMO	4.4252	280.18	0.1213	0.62137
		HOMO→LUMO+1	5.5991	221.44	0.3985	0.55812
MeCN	6-31G(d)	HOMO→LUMO	3.8787	319.65	0.0878	0.62921
		HOMO-1→LUMO	4.5099	274.92	0.1102	0.61828
		HOMO→LUMO+1	5.7619	215.18	0.3577	0.56192
	6-311G(d,p)	HOMO→LUMO	3.8673	320.59	0.0903	0.63197
		HOMO-2→LUMO	4.5046	275.24	0.1112	0.61913
		HOMO→LUMO+1	5.7142	216.98	0.3777	0.55622
	6-31+G(d,p)	HOMO→LUMO	3.8152	324.98	0.0929	0.63165
		HOMO-1→LUMO	4.4154	280.80	0.1237	0.62082
		HOMO→LUMO+1	5.6022	221.31	0.4159	0.56150
	6-311++G(d,p)	HOMO→LUMO	3.8180	324.73	0.0923	0.63257
		HOMO-1→LUMO	4.4234	280.29	0.1216	0.62139
		HOMO→LUMO+1	5.5992	221.43	0.3990	0.55936

6-31G(d) ; 6-311G(d,p) ; 6-31+G(d,p) and 6-311++G(d,p) correspond, in the text, to B; B2; B1 and B3 respectively.

Table 5. Energies gap ΔE (eV) ($\Delta E = E_{\text{LUMO}} - E_{\text{HOMO}}$), calculated absorption wavelengths λ (nm) of **CH₃Q** in gas phase and in solution. Only the three first transitions with an oscillator strength (f)>0.1 and CI expansion coefficient >48% are reported.

CH ₃ Q	Basis set	Excitations	ΔE (eV)	λ (nm)	f	CI expansion coefficient
Gas	6-31G(d)	HOMO→LUMO	4.0235	308.15	0.1345	0.62656
		HOMO-2→LUMO	4.6288	267.85	0.1129	0.61474
		HOMO→LUMO+1	5.6978	217.60	0.2688	0.50786
	6-311G(d,p)	HOMO-1→LUMO	4.0185	308.54	0.1399	0.62873
		HOMO-2→LUMO	4.6197	268.38	0.1137	0.61415
		HOMO→LUMO+1	5.6521	219.36	0.2803	0.50005
	6-31+G(d,p)	HOMO→LUMO	3.9670	312.54	0.1486	0.62823
		HOMO-2→LUMO	4.5357	273.35	0.1225	0.61748
		HOMO→LUMO+1	5.5485	223.46	0.2946	0.48383
	6-311++G(d,p)	HOMO→LUMO	3.9741	311.98	0.1470	0.62916
		HOMO-2→LUMO	4.5420	272.97	0.1207	0.61786
		HOMO→LUMO+1	5.5438	223.65	0.2802	0.48030
THF	6-31G(d)	HOMO→LUMO	4.0046	309.61	0.1262	0.62503
		HOMO-2→LUMO	4.5630	271.72	0.1236	0.61922
		HOMO→LUMO+1	5.7067	217.26	0.2683	0.55110
	6-311G(d,p)	HOMO→LUMO	4.0027	309.75	0.1323	0.62760
		HOMO-2→LUMO	4.5633	271.70	0.1237	0.61961
		HOMO→LUMO+1	5.6591	219.09	0.2782	0.54260
	6-31+G(d,p)	HOMO→LUMO	3.9502	313.87	0.1394	0.62654
		HOMO-1→LUMO	4.4726	277.21	0.1345	0.62192
		HOMO→LUMO+1	5.5587	223.04	0.2934	0.54250
	6-311++G(d,p)	HOMO→LUMO	3.9572	313.31	0.1384	0.62762
		HOMO-1→LUMO	4.4823	276.61	0.1321	0.62251
		HOMO→LUMO+1	5.5530	223.27	0.2779	0.54054
EtOH	6-31G(d)	HOMO→LUMO	3.9995	310.00	0.1246	0.62498
		HOMO-1→LUMO	4.5527	272.33	0.1248	0.61960
		HOMO→LUMO+1	5.7080	217.21	0.2696	0.55688
	6-311G(d,p)	HOMO→LUMO	3.9982	310.10	0.1308	0.62761
		HOMO-2→LUMO	4.5546	272.22	0.1248	0.62014
		HOMO→LUMO+1	5.6601	219.05	0.2797	0.54848
	6-31+G(d,p)	HOMO→LUMO	3.9457	314.22	0.1376	0.62647
		HOMO-1→LUMO	4.4631	277.80	0.1359	0.62225
		HOMO→LUMO+1	5.5600	222.99	0.2954	0.55036
	6-311++G(d,p)	HOMO→LUMO	3.9527	313.67	0.1367	0.62755
		HOMO-1→LUMO	4.4731	277.18	0.1334	0.62288
		HOMO→LUMO+1	5.5542	223.23	0.2798	0.54851
MeCN	6-31G(d)	: HOMO→LUMO	3.9987	310.06	0.1243	0.62498
		HOMO-1→LUMO	4.5512	272.42	0.1250	0.61966
		HOMO→LUMO+1	5.7081	217.21	0.2699	0.55775
	6-311G(d,p)	HOMO→LUMO	3.9975	310.16	0.1306	0.62762
		HOMO-2→LUMO	4.5532	272.30	0.1249	0.61954
		HOMO→LUMO+1	5.6602	219.05	0.2800	0.54937
	6-31+G(d,p)	HOMO→LUMO	3.9450	314.28	0.1373	0.62646
		HOMO-1→LUMO	4.4616	277.89	0.1361	0.62230
		HOMO→LUMO+1	5.5602	222.99	0.2958	0.55154
	6-311++G(d,p)	HOMO→LUMO	3.9520	313.73	0.1364	0.62755
		HOMO-1→LUMO	4.4717	277.26	0.1336	0.62293
		HOMO→LUMO+1	5.5544	223.22	0.2801	0.54970

6-31G(d) ; 6-311G(d,p) ; 6-31+G(d,p) and 6-311++G(d,p) correspond, in the text, to B; B2; B1 and B3 respectively.

Table 6. Energies gap ΔE (eV) ($\Delta E = E_{\text{LUMO}} - E_{\text{HOMO}}$), calculated absorption wavelengths λ (nm) of **CHOQ** in gas phase and in solution. Only the three first transitions with an oscillator strength (f) >0.1 and CI expansion coefficient $>40\%$ are reported.

CHOQ	Basis set	Excitations	ΔE (eV)	λ (nm)	f	CI expansion coefficient
Gas	6-31G(d)	HOMO-1→LUMO	3.3151	374.00	0.0972	0.64033
		HOMO-2→LUMO	4.1941	295.62	0.2087	0.61939
		HOMO-1→LUMO+2	5.3240	232.88	0.0573	0.41602
	6-311G(d,p)	HOMO-1→LUMO	3.3318	372.12	0.0997	0.64222
		HOMO-2→LUMO	4.2016	295.09	0.2095	0.62067
		HOMO-1→LUMO+2	5.2810	234.77	0.0535	0.43936
	6-31+G(d,p)	HOMO→LUMO	3.2754	378.53	0.1016	0.64236
		HOMO-2→LUMO	4.1211	300.85	0.2272	0.62177
		HOMO→LUMO+2	5.1848	239.13	0.0600	0.43350
	6-311++G(d,p)	HOMO→LUMO	3.2974	376.00	0.1016	0.64298
		HOMO-2→LUMO	4.1396	299.51	0.2246	0.62214
		HOMO→LUMO+2	5.1852	239.11	0.0476	0.46211
THF	6-31G(d)	HOMO→LUMO	3.2206	384.97	0.0796	0.64080
		HOMO-2→LUMO	4.0647	305.03	0.2400	0.61746
		HOMO→LUMO+1	5.3351	232.39	0.0599	0.39071
	6-311G(d,p)	HOMO→LUMO	3.2403	382.64	0.0822	0.64261
		HOMO-2→LUMO	4.0763	304.16	0.2410	0.61937
		HOMO→LUMO+1	5.3088	233.54	0.0591	0.39971
	6-31+G(d,p)	HOMO→LUMO	3.1830	389.52	0.0812	0.64315
		HOMO-2→LUMO	3.9908	310.68	0.2628	0.61926
		HOMO→LUMO+1	5.2131	237.83	0.1087	0.47714
	6-311++G(d,p)	HOMO→LUMO	3.2043	386.93	0.0819	0.64356
		HOMO-2→LUMO	4.0120	309.03	0.2587	0.61983
		HOMO→LUMO+1	5.2240	237.33	0.0978	0.45988
EtOH	6-31G(d)	HOMO→LUMO	3.2016	387.25	0.0765	0.64101
		HOMO-2→LUMO	4.0435	306.63	0.2447	0.61685
		HOMO→LUMO+1	5.3301	232.61	0.0654	0.40598
	6-311G(d,p)	HOMO→LUMO	3.2222	384.78	0.0791	0.64279
		HOMO-2→LUMO	4.0557	305.71	0.2458	0.61882
		HOMO→LUMO+1	5.3073	233.61	0.0668	0.41867
	6-31+G(d,p)	HOMO→LUMO	3.1640	391.86	0.0776	0.64342
		HOMO-2→LUMO	3.9699	312.31	0.2678	0.61855
		HOMO→LUMO+1	5.2041	238.24	0.1368	0.51984
	6-311++G(d,p)	HOMO→LUMO	3.1858	389.18	0.0784	0.64378
		HOMO-2→LUMO	3.9916	310.61	0.2636	0.61913
		HOMO→LUMO+1	5.2165	237.68	0.1339	0.51701
MeCN	6-31G(d)	HOMO→LUMO	3.1986	387.63	0.0760	0.64105
		HOMO-2→LUMO	4.0402	306.88	0.2454	0.61676
		HOMO→LUMO+1	5.3291	232.65	0.0666	0.40897
	6-311G(d,p)	HOMO→LUMO	3.2193	385.13	0.0786	0.64282
		HOMO-2→LUMO	4.0524	305.95	0.2465	0.61873
		HOMO→LUMO+1	5.3068	233.63	0.0683	0.42227
	6-31+G(d,p)	HOMO→LUMO	3.1609	392.25	0.0770	0.64347
		HOMO-2→LUMO	3.9667	312.57	0.2686	0.61844
		HOMO→LUMO+1	5.2021	238.33	0.1415	0.52650
	6-311++G(d,p)	HOMO→LUMO	3.1828	389.55	0.0778	0.64383
		HOMO-2→LUMO	3.9884	310.86	0.2643	0.61902
		HOMO→LUMO+1	5.2146	237.76	0.1399	0.52564

6-31G(d) ; 6-311G(d,p) ; 6-31+G(d,p) and 6-311++G(d,p) correspond, in the text, to B; B2; B1 and B3 respectively.

For the quinoxaline derivatives, the extension of the basis set produce a slight bathochromic shifts estimated by 5 to 6 nm as difference between the λ_{\max} calculated using the less and the most extended basis (6-31G(d) (B) and 6-311++G(d,p) (B3)) in vacuum and in the three polar solvents considered in this work. To sum up, the theoretical calculations of the electronic spectrum with extended basis 6-311++G (d,p) containing—diffuse orbitals gave results in better agreement with the experiment.

A hypochromic shift is clearly noticed on the UV spectrum of the **CHOQ** compound for the absorption band intensity at 237.7 nm (using B3 in EtOH), this shift is the most important compared to the two other peaks at 310.6 and 389.2 nm (see Fig. 4 and Table 6). While a slight hypochromic shift appears on the two absorption bands at larger wavelengths λ_{\max} for **HQ** and **CH₃Q** (Fig. 4, Tables 4 and 5). There is almost no effect of the solvent on the most intense peak centered at the shortest one (221.8 and 223.7 nm for **HQ** and **CH₃Q** respectively).

A bathochromic shift on the two larger absorption bands due to the solvent effect is noticed for the studied compounds. This shift is more important for **CHOQ** and increase with the solvent polarity for the three quinoxaline derivatives. Moreover, one can notice weak hypsochromic shifts in the shorter wavelength (λ_{\max}) (See Tables 4-6). Considering the results obtained using B3 in the vacuum and in MeCN solvent which is the most polar of the three solvents used in this work since its dielectric constant is higher than those of EtOH and THF. Therefore, it is possible to evaluate the bathochromic or hypsochromic shifts due to the solvent as a difference between the wavelength values (λ_{\max}) in the vacuum and in the presence of the solvent. For bathochromic shifts, this difference is estimated for the tow larger values of λ_{\max} at 3 and 6 nm, 2 and 4nm and 13.6 and 11.4 nm for **HQ**, **CH₃Q** and **CHOQ** respectively, while the hypsochromic shift is evaluated by 0.4 nm for **HQ** and **CH₃Q** molecules and 1.3 nm for **CHOQ** molecule. In many aspects, an obvious effect of the solvent polarity on the electronic spectra of the studied compound is highlighted especially for **CHOQ** compound.

For **HQ** the three first absorption peaks at 324.6, 280.2 and 221.4 nm obtained with B31YP/B3 in EtOH (Table 4 and Fig. 4(a)) are in good agreement with the experimental UV spectrum given in Fig.1 which shows absorption bands at 350, 280 and 230 nm respectively. However, the difference between the theoretical and experimental λ_{\max} values for the absorption bands at 324.6 and 221.4 are 15 and 8 nm respectively less than 20nm obtained by N. Prabavathi et al.⁴⁸. The long-wavelength absorption transition at 324.6 nm could be assigned to the HOMO→LUMO transition (contribution of 63%, Table 4). The HOMO has a pronounced π character

localized on the quinoxaline moiety and on the oxygen atom of the carboxyl group of **HQ**, whereas the LUMO has antibonding π character (Fig. 3). The HOMO→LUMO transition is then characterized as a $\pi \rightarrow \pi^*$ electronic transition. The calculated absorption band at 280.2 nm could be attributed to HOMO-1→LUMO transition with a contribution of 62% (Table 4). The isodensity surface plots of the molecular orbitals (MOs) (Fig. 3) show that the HOMO-1 has a π character on the benzene ring, thus, this band is assigned also to $\pi \rightarrow \pi^*$ transition.

In the theoretical electronic spectrum of **CH₃Q** molecule obtained in EtOH and with 6-311++G(d,p) (B3) as a basis set, the absorption bands appear at 313.7, 277.2 and 223.2 nm (Table 5 and Fig. 4 (b)). The absorption peak at 313.67 nm could probably be attributed to HOMO→LUMO excitation with a contribution of 0.63%, The HOMO has a pronounced π character localized on π -system of quinoxaline moiety while the LUMO has antibonding π character mostly localized on the quinoxaline moiety (Fig. 3); therefore, this excitation is attributed to π - π^* transition. The absorption peak at 277.2 nm involves the HOMO-1→LUMO excitation with a contribution of 62%, the isodensity plots of the HOMO-1 (Fig. 3) shows a pronounced π -character on the benzene, this electronic excitation is assigned to π - π^* transition mainly localized on the benzene ring. The last wavelength at 223.2 nm corresponds to the HOMO→LUMO+1 excitation with 55% as a contribution in the IC function, moreover, LUMO+1 present a pronounced antibonding character with a high electronic density on the π -system of the benzene, as a consequence this excitation is assigned to π - π^* transition.

Table 6 and Fig. 4 (c), show three λ_{\max} values calculated at 389.2, 310.6 and 237.7 nm for **CHOQ** derivative, the major IC coefficients show that these peaks can correspond to HOMO→LUMO, HOMO-2→LUMO and HOMO→LUMO+1 excitations respectively. The electronic density (Fig. 3) allows to deduce that these excitations are assigned to π - π^* transition since the HOMO present a high density on the quinoxaline ring, the HOMO-2 is localized on N atomic centers and on the benzene ring. The LUMO and LUMO+1 present an anti-bonding π character localized on the quinoxaline ring and on benzene ring respectively. To conclude, the three calculated absorption bands are mainly derived from the contribution of excitations due to π - π^* transition. The comparison between **HQ** and **CH₃Q** results (Tables 4-5) shows an undergo hypsochromic shifts on the three absorption bands. For the theoretical band calculated at 321.8 and 324.6 nm for **HQ** in a vacuum and EtOH and using 6-311++G (d, p) basis, this shift is evaluated by 10 and 11 nm in vacuum and in EtOH respectively. For two other peaks, calculated in EtOH and using 6-311++G (d,p), at 280.2 and 221.4 nm, this hypsochromic shifts is

weak and estimated to 3 and 2 nm respectively. A bathochromic shift caused by the substitution of the H in **HQ** by CHO group is deduced from the results given in Tables 6 and Fig. 4. In EtOH and using 6-311++G (d,p), this shift is strong and estimated to 65 nm for the peak at 324.6, while it is evaluated by 30 and 16 nm for the absorption bands at 280.2 and 221.4 nm respectively. One can notice a hypochromic effect on the three band intensities due to the substitution of H in **HQ** by CH₃; while a hyperchromic effect is observed on the three peaks when one replace H in **HQ** by CHO group.

Conclusion

The geometrically optimized structures of **HQ**, **CH₃Q** and **CHOQ** show that the bond distances and bond angles related to quinoxaline rings are in good agreement with the experiment. The use 6-31G* is sufficient to well describe the geometrical structure of quinoxaline derivatives. However, the addition of the diffuse functions in the basis is necessary to improve the theory-experiment approach concerning the evaluation of the excitation energies.

The most important energetic stabilization caused by the solvent polarity is observed for **CHOQ** compound.

The calculated excitation energies using TD-B3LYP underestimate or overestimate the experimental values, therefore this method fail to reproduce the experimentally estimated excitation energies.

The most bathochromic and hypsochromic shifts on the λ_{\max} values are clearly observed for **CHOQ** compound, in the UV spectrum, due to the strong effect of solvent polarity. Indeed, the bathochromic effect is observed for the two larger λ_{\max} values and the major hypsochromic effect is noticed for the shorter wavelength value of λ_{\max} .

The calculated UV absorption maxima at 324.6, 280.2 and 221.4 nm, obtained for **HQ** using extended basis sets containing diffuse orbitals in EtOH as the solvent, is in good agreement with the experiment. The three absorption bands are derived from the contribution of the excitations due to π - π^* transitions. From the electronics spectra of **HQ**, **CH₃Q** and **CHOQ**, one can deduce that the substitution of H in **HQ** by CH₃ group (electro-donor) cause an undergo hypsochromic shift on λ_{\max} values. While the substitution of H by CHO (electro-attractor) occurs a bathochromic shift in wavelength associated to the absorption maximum. A hypochromic and hyperchromic effects are clearly noticed on the absorption band when we replace H in **HQ** by CH₃ and CHO group respectively. Thus it is possible to establish a direct relationship between the nature of substituent group (electro-donor/attractor) and the different effects on the displacement and intensity of the absorption bands observed in the UV spectra of quinoxaline derivatives.

References

- 1- V. Krishnakumar, N. Prabavathi, Spectrochim. Acta, Part A, **2010**, 77, 238-247.
- 2- H. Kinashi, S.L. Otten, J.S. Duncan, C.R. Hutchinson, J. Antibiot., **1988**, 41 624-637.
- 3- R. Sarges, H.R. Howard, R.G. Browne, L.A. Lebel, P.A. Seymour, B.K. Koe, J. Med. Chem., **1990**, 33, 2240-2254.
- 4- W. Loshner, H. Lehmann, B. Behl, W. Lubish, T. Hoger, H.G. Lemair, G. Gross, Eur. J. Neurosci., **1999**, 11, 250-262.
- 5- P. Sanna, A. Carta, M. Loriga, S. Zanetti, L. Sechi, Il Farmaco, **1998**, 53, 455-461.
- 6- Y.B. Kim, Y.H. Kim, J.Y. Park, S.K. Kim, Bioorg. Med. Chem. Lett., **2004**, 14, 541-544.
- 7- S.T. Hazeldine, L. Polin, J. Kushner, K. White, T.H. Corbett, J. Biehl, J.P. Horwitz, Bioorg. Med. Chem., **2005**, 13, 1069-1081.
- 8- S.T. Hazeldine, L. Polin, J. Kushner, K. White, T.H. Corbett, J. Biehl, J.P. Horwitz, Bioorg. Med. Chem., (2005), 13, 3910-3920.
- 9- S.T. Hazeldine, L. Polin, J. Kushner, K. White, N.M. Bouregeois, B. Crantz, E. Palomino, T.H. Corbett, J. Biehl, J.P. Horwitz, Bioorg. Med. Chem., **2002**, 45 3130-3137.
- 10- S.T. Hazeldine, L. Polin, J. Kushner, J. Paluch, K. White, M. Edelstein, E. Palomino, T.H. Corbett, J.P. Horwitz, Bioorg. Med. Chem., **2001**, 44, 1758-1776.
- 11- Y. Ikeda, E. Kuwano, M. Eto, J. Fac. Agric., **1992**, 37, 81-92.
- 12- Y. Ura, G. Sakata, K. Makino, T. Ikai, Y. Kawamura, German Offenlegungsschrift DE, 3004770.
- 13- N.T. Ghoms, N.H. Ahabchane, N. Es-Safi, B. Garrigues, E.M. Essasi, Spectrosc. Lett., **2007**, 40, 741-751.
- 14- D. Rose, E. Liesk, H. Hoeffkes, K.-G. A. Hengel, German Offenlegungsschrift DE, **1999**, 3, 212.
- 15- K. Toshima, R. Takano, T. Ozawa, S. Matsumura, J. Chem. Soc. Chem. Commun., **2002**, 212-213. DOI: 10.1039/B107829C.
- 16- G. Ughetto, A.H.J. Wang, G.J. Quigley, G.A. Van Der Marel, J.H. Van Boom, A. Rich, Nucleic Acids Res., **1985**, 13, 2305-2323.
- 17- M.A. Viswamitra, O. Kennard, W.B.T. Cruse, E. Egert, G.M. Sheldrick, P.G. Jones, M.J. Waring, L.P.G. Wakelin, R.K. Olsen, Nature (London), **1981**, 289, 817.
- 18- M.A. Palafox, G. Tardajos, A.G. Martines, V.K. Rastogi, D. Mishra, S.P. Ojha, W. Kiefer, Chem. Phys., **2007**, 340, 17-31.
- 19- N.C. Handy, P.E. Masley, R.D. Amos, J.S. Andrews, C.W. Murray, G. Laming, Chem. Phys. Lett., **1992**, 197, 506-515.
- 20- N.C. Handy, C.W. Murray, R.D. Amos, J. Phys. Chem., **1993**, 97, 4392-4396.
- 21- P.J. Stephens, F.J. Devlin, C.F. Chavalowski, M.J. Frisch, J. Phys. Chem., **1994**, 98, 11623-11627.

- 22- F.J. Devlin, J.W. Finley, P.J. Stephens, M.J. Frisch, *J. Phys. Chem.*, **1995**, 99, 16883-16902.
- 23- J.-P. Cornard, C. Lapouge, *Chem. Phys. Lett.*, **2007**, 438, 41-47.
- 24- J.-P. Cornard, C. Lapouge, J.-C. Merlin, *Chem. Phys.*, **2007**, 340, 273-282.
- 25- Ş. Yurdakul, T. Polat, *J. Mol. Struct.*, **2010**, 963, 194-201.
- 26- N. Padjama, S. Ramakumar, M.A. Viswamitra, *Acta Cryst. C*, **1987**, 43, 2239-2240.
- 27- N. Prabavathi, A. Nilufer, V. Krishnakumar, *Spectrochim. Acta, Part A*, **2012**, 92, 325- 335.
- 28- S.M. Soliman, J. Albering, M.A.M. Abu-Youssef, *J. Mol. Struct.*, **2013**, 1053, 48-60.
- 29- S. Badoğlu, Ş. Yurdakul, *Spectrochim. Acta, Part A*, **2013**, 101, 14-21.
- 30- Rajratna P. Tayade, Nagaiyan Sekar, *J. Lumin.*, **2016**, 176, 298-308.
- 31- S. Sebastian, S. Sylvestre, J. Jayabharathi, S. Ayyapan, M. Amalanathan, K. Oudayakumar, Ignatius A. Herman, *Spectrochimica Acta Part A*, **2015**, 136, 1107-1118.
- 32- Y. S. Hong, H. M. Kim, Y.T. Park, H. S. Kim, *Bull. Korean Chem. Soc.*, **2000**, 21, 133-136.
- 33- A.D. Becke, *J. Chem. Phys.*, **1992**, 96, 9489-9495.
- 34- A.D. Becke, *J. Chem. Phys.*, **1993**, 98, 1372-1377.
- 35- C. Lee, W. Yang, R.G. Parr, *Phys. Rev. B*, **1988**, 37, 785-789.
- 36- M.J. Frisch, G.W. Trucks, H.B. Schlegel, G.E. Scuseria, M.A. Robb, J.R. Cheeseman, J.A. Montgomery, Jr., T. Vreven, K.N. Kudin, J.C. Burant, J.M. Millam, S.S. Iyengar, J. Tomasi, V. Barone, B. Mennucci, M. Cossi, G. Scalmani, N. Rega, G.A. Petersson, H. Nakatsuji, M. Hada, M. Ehara, K. Toyota, R. Fukuda, J. Hasegawa, M. Ishida, T. Nakajima, Y. Honda, O. Kitao, H. Nakai, M. Klene, X. Li, J.E. Knox, H.P. Hratchian, J.B. Cross, C. Adamo, J. Jaramillo, R. Gomperts, R.E. Stratmann, O. Yazyev, A.J. Austin, R. Cammi, C. Pomelli, J.W. Ochterski, P.Y. Ayala, K. Morokuma, G.A. Voth, P. Salvador, J.J. Dannenberg, V.G. Zakrzewski, S. Dapprich, A.D. Daniels, M.C. Strain, O. Farkas, D.K. Malick, A.D. Rabuck, K. Raghavachari, J.B. Foresman, J.V. Ortiz, Q. Cui, A.G. Baboul, S. Clifford, J. Cioslowski, B.B. Stefanov, G. Liu, A. Liashenko, P. Piskorz, I. Komaromi, R.L. Martin, D.J. Fox, T. Keith, M.A. Al-Laham, C.Y. Peng, A. Nanayakkara, M. Challacombe, P.M.W. Gill, B. Johnson, W. Chen, M.W. Wong, C. Gonzalez, J.A. Pople, Gaussian 03, Revision B.01, Gaussian, Inc., Pittsburgh, PA, **2003**.
- 37- J.B. Foresman, T.A. Keith, K.B. Wiberg, J. Snoodian, M.J. Frisch, *J. Phys. Chem.*, **1996**, 100, 16098-16104.
- 38- G.A. Jaffrey, *An Introduction to Hydrogen Bonding*, Oxford University Press, **1997**, 32.
- 39- S. Sudha, N. Sundaraganesan, K. Vanchinathan, K. Muthu, SP. Meenakshisundaram, *J. Mol. Struct.*, **2012**, 1030, 191-203.
- 40- R.M. Issa, M.K. Awad, F.M. Atlam, *Appl. Surf. Sci.*, **2008**, 255, 2433-2441.
- 41- D. Jacquemin, J. Preat, E.A. Perpète, *Chem. Phys. Lett.*, **2005**, 410, 254-259.
- 42- D. Jacquemin, J. Preat, M. Charlot, V. Wathelet, J.M. Andre, E.A. Perpète, *J. Chem. Phys.*, **2004**, 121, 1736-1743.
- 43- M. Cossi, V. Barone, *J. Chem. Phys.*, **2001**, 115, 4708-4717.
- 44- T. Minami, M. Nakano 17th June 2016, F. Castet, *J. Phys. Chem. Lett.*, **2011**, 2, 1725-1730.
- 45- K. Okuno, Y. Shigeta, R. Kishi, M. Nakano, *Chem. Phys. Lett.*, 585 (2013) 201-206.
- 46- R. Baer, I.E. Livshits, U. Salzner, *Rev. Phys. Chem.*, 61 (2010) 85-109.
- 47- T. Stein, H. Eisenberg, L. Kronik, R. Baer, *Phys. Rev. Lett.*, **2010**, 105, 266802
- 48- N. Prabavathi, A. Nilufer, V. Krishnakumar, *Spectrochim. Acta, Part A*, **2014**, 121, 483-493.